THE JOURNAL OF PHYSICAL CHEMISTRY B
A JOURNAL OF THE AMERICAN CHEMICAL SOCIETY

pubs.acs.org/JPCB
Article

Local and Large-Scale Conformational Dynamics in Unfolded Proteins and IDPs. I. Effect of Solvent Viscosity and Macromolecular Crowding

Karin Stecher,[#] Florian Krieger,[#] Michael Schleeger, and Thomas Kiefhaber*

Cite This: J. Phys. Chem. B 2023, 127, 8095–8105
Read Online

ABSTRACT: Protein/solvent interactions largely influence protein dynamics, particularly motions in unfolded and intrinsically disordered proteins (IDPs). Here, we apply triplet-triplet energy transfer (TTET) to investigate the coupling of internal protein motions to solvent motions by determining the effect of solvent viscosity (η) and macromolecular crowding on the rate constants of loop formation (k_c) in several unfolded polypeptide chains including IDPs. The results show that the viscosity dependence of loop formation depends on amino acid sequence, loop length, and co-solute size. Below a critical size (r_c), co-solutes exert a maximum effect, indicating that under these conditions microviscosity experienced by chain motions matches macroviscosity of the solvent. r_c depends on chain stiffness and reflects the length scale of the chain motions, i.e., it is related to the persistence length. Above r_c, the effect of solvent viscosity decreases with increasing co-solute size. For co-solutes typically used to mimic cellular environments, a scaling of $k_c \propto \eta^{-0.1}$ is observed, suggesting that dynamics in unfolded proteins are only marginally modulated in cells. The effect of solvent viscosity on k_c in the small co-solute limit (below r_c) increases with increasing chain length and chain flexibility. Formation of long and very flexible loops exhibits a $k_c \propto \eta^{-1}$ viscosity dependence, indicating full solvent coupling. Shorter and less flexible loops show weaker solvent coupling with values as low as $k_c \propto \eta^{-0.75 \pm 0.02}$. Coupling of formation of short loops to solvent motions is very little affected by amino acid sequence, but solvent coupling of long-range loop formation is decreased by side chain sterics.

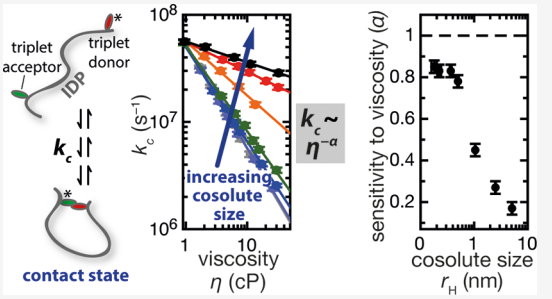

INTRODUCTION

Solvent motions coupled to internal protein motions are the basis for dynamic processes in proteins and are essential for protein folding and function.[1−3] Studies on the native state of proteins revealed different types of dynamic modes. Large-scale protein motions in myoglobin were shown to be inversely proportional to solvent viscosity, i.e., they are fully coupled to solvent dynamics (α-fluctuations) and are thus based on interactions of the protein with the bulk solvent.[1,4] Local motions, in contrast, were observed to be independent of bulk solvent viscosity and were assigned to interactions of the solvation shell with the protein (β-fluctuations).[4,5] The coupling of solvent motions to the dynamics in the unfolded state of proteins is much less understood, although it is important for the understanding of the dynamics in unfolded polypeptide chains like intrinsically disordered proteins (IDPs) and the early steps in protein folding. Chain motions in unfolded proteins should be largely influenced by interactions of the solvent with the amide backbone, which leads to much larger conformational fluctuations than dynamics in native proteins, due to the larger flexibility and the increased conformational space available for an unfolded polypeptide chain. To understand the contributions of solvent dynamics to both local and large-scale motions in unfolded proteins, we investigated the effect of solvent viscosity on the conformational dynamics in unfolded polypeptide chains of different length and amino acid sequence, including sequences from IDPs.

Several studies have addressed the coupling of solvent motions to polypeptide chain dynamics by investigating the effect of solvent viscosity on the internal dynamics in unfolded polypeptide chains, but gave contradictory results. Generally, the effect of solvent viscosity (η) on dynamic processes with the rate constant k in solution can be described by

$$k = k_0 \left(\frac{\eta}{\eta_0} \right)^{-\alpha} \quad (1)$$

where η_0 is the reference solvent viscosity, typically of water at room temperature, and k_0 is the rate constant at η_0. α reflects the sensitivity of the dynamics to solvent viscosity with the

Received: June 16, 2023
Revised: August 23, 2023
Published: September 18, 2023

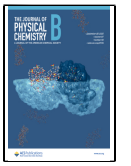

https://doi.org/10.1021/acs.jpcb.3c04070
J. Phys. Chem. B 2023, 127, 8095−8105

limiting values of $\alpha = 1$ for a $1/\eta$ viscosity dependence, corresponding to a Kramer's-type behavior,[6] and $\alpha = 0$ for a reaction that is insensitive to solvent viscosity. Sauer and co-workers used photoinduced electron transfer (PET) on poly(Gly-Ser) chains and proposed a $1/\eta$ viscosity dependence ($\alpha = 1$) for loop formation, independent of loop length.[7] Work on loop formation dynamics using tryptophan triplet quenching by cysteine, which is not diffusion-controlled, also assumed a $1/\eta$ viscosity dependence for all chains. This value was used to extrapolate the rate constant for loop formation, k_c, from the viscosity dependence of the measured apparent rate constants.[8,9] An α-value of 1 was also assumed in single molecule fluorescence correlation spectroscopy experiments on the effect of solvent viscosity on reconfiguration times in unfolded proteins.[10] On the other hand, diffusion-controlled triplet-triplet energy transfer (TTET) experiments showed a $1/\eta$ viscosity dependence ($\alpha = 1$) for a long and flexible poly(Gly-Ser) loop but revealed a weaker viscosity dependence with α-values as low as 0.75 for a short poly(Gly-Ser) loop[11] and for stiffer, proline containing loops.[12] Experimental results on internal dynamics in the synthetic linear polymers 1,2-polybutadiene, polystyrene, and polyisoprene measured both by NMR and by time-resolved optical spectroscopy also showed a weaker viscosity dependencies for local polymer dynamics with α-values between 0.41 and 0.86, indicating that local chain motions in these polymers are not fully coupled to solvent dynamics.[13−18] These findings are supported by MD simulations on the dynamics in short peptides that found α-values <1, which were interpreted to be due to local steric barriers for backbone rotations.[19] Further, theoretical considerations on the dynamics of loop formation in polymers also suggested α-values <1 due to a breakdown of the local thermal equilibrium approximation.[20] These results from experiments, simulations, and theory suggest that local dynamics in unfolded proteins are not fully coupled to solvent dynamics and thus may not exhibit a $1/\eta$ viscosity dependence.

The different results obtained for the effect of solvent-viscosity on internal dynamics in unfolded polypeptide chains may be due to the application of different methods, which are sensitive to either local or large-scale dynamics, to different peptide sequences, and/or to the use of different co-solutes to modulate solvent viscosity. We therefore studied the viscosity dependence of the dynamics of intrachain loop formation in polypeptide chains of different length and amino acid sequence in the presence of various co-solutes. This gives a detailed picture of the coupling of solvent motions to local and large-scale internal motions in unfolded proteins and its dependence on the nature of the co-solutes.

Intrachain loop formation leads to site-specific interactions within the polypeptide chain and is thus an elementary step in protein folding that determines how fast conformational space can be explored in search for energetically favorable conformations. Our group has previously used TTET between xanthone (Xan) as the triplet donor and naphthylalanine (Nal) as the triplet acceptor group to study the dynamics of site-specific contact formation in unfolded model polypeptide chains of different lengths[11,12,21−23] and in a naturally occurring protein loop.[24] TTET between Xan and Nal is a fast and diffusion-controlled two electron transfer process (Dexter mechanism) that is based on van der Waals contact between Xan and Nal with a reactive boundary of 4.4 Å.[25] When the donor and acceptor are attached to a polypeptide chain, the transfer kinetics directly reflect the rate constant for formation of a loop (k_c) that brings donor and acceptor into van der Waals distance. The time resolution of this method is set by the photophysics of triplet formation and triplet transfer, which both occur in the range of 2−3 ps.[26,27] The upper time limit for processes that can be monitored by TTET is given by the lifetime of the Xan triplet state, which is about 50 μs in water.[22] Characterization of intrachain loop formation in unfolded poly(Gly-Ser) and polyserine model polypeptide chains by TTET revealed different scaling of the rate constant for loop formation with loop length for local and long-range loop formation.[22] The time constant ($1/k_c$) for formation of short loops is almost independent of chain length and reaches a limiting value of 5 ns for flexible poly(Gly-Ser) chains at 22.5 °C. For long poly(Gly-Ser)$_n$ chains with $n > 8$, loop formation scales with $N^{-1.7 \pm 0.1}$, where N is the number of amino acids in the loop. A similar behavior was found for loop formation in stiffer polyserine chains with slightly reduced rate constants and a two-fold slower limiting rate constant for short chains.[22] In addition, very fast loop formation reactions on the hundreds of picoseconds time scale were detected in a subpopulation of the molecules, especially for formation of short loops.[23] The factors determining the dynamics in the different regimes for local and long-range loop formation are still not well understood, but the observed scaling behavior suggests that formation of long loops represents a diffusive search of a Gaussian chain with excluded volume, whereas formation of short loops contains contributions from chain stiffness.[22]

Here, we investigated the effect of solvent viscosity on loop formation dynamics in homopolypeptide chains of different loop lengths and amino acid sequences to characterize solvent effects on both local dynamics that occur within the persistence length of the polypeptide chain and on long-range dynamics that require large-scale chain motions. In addition, we investigated viscosity effects on the dynamics of three fragments from IDPs and of a short natural protein turn region from hairpin 1 of protein G (GB1 hairpin). By varying the co-solute, we further tested for differences between the effect of small and large co-solutes to relate the macroscopic solvent viscosity to the microscopic viscosity experienced by chain dynamics both for local and large-scale motions. Varying the co-solute size further enabled us to assess the effect of large macromolecular crowding agents on local and large-scale conformational dynamics to gain information on the effect of a cellular environment on the dynamics of unfolded proteins and peptides.

MATERIALS AND METHODS

Peptide Synthesis and Purification. All peptides were synthesized using standard fluorenylmethoxycarbonyl (Fmoc) chemistry on preloaded resins from Rapp Polymer (Tübingen, Germany). 9-Oxoxanthen-2-carboxylic acid was synthesized as described[28] and attached to the N-terminus of the peptides using Fmoc chemistry. Peptides were purified by reversed-phase HPLC, and purity of all peptides was checked by mass spectroscopy and analytical HPLC.

Sample Preparation and Characterization. Peptide concentrations were determined by UV absorbance at 343 nm using a molar absorption coefficient of 3900 M^{-1} cm^{-1} for xanthone in water. Solvent viscosity was changed by adding various amounts of co-solutes. The maximum weight fractions for the different co-solutes were as follows: Ficoll (23% w/w), PEG 20000 (18% w/w), PEG 6000 (35% w/w), PEG 1500 (31% w/w), PEG 1000 (44% w/w), PEG 600 (48% w/w),

https://doi.org/10.1021/acs.jpcb.3c04070
J. Phys. Chem. B 2023, 127, 8095−8105

PEG 400 (43% w/w), sucrose (57% w/w), glucose (61%), glycerol (71% w/w), ethylene glycol (90% w/w), and urea (41% w/w). Solvent viscosity was measured for each solution in a HAAKE falling-ball viscosimeter Type C from Thermo Scientific. Random coil conformation was confirmed for all peptides at all co-solute concentrations by CD experiments. This is in accordance to recent experimental results, which showed the absence of interactions between PEG-based co-solutes/ethylene glycol and unfolded proteins.[29] CD measurements were carried out on an AVIV 62ADS or an AVIV 410 spectropolarimeter (AVIV, Lakewood, NJ, USA). Absorbance and fluorescence measurements were performed with a ChronosFD spectrometer (ISS) or an AMINCO Bowman series 2 spectrofluorimeter (SLM Aminco).

Laser Flash Photolysis Experiments. Transient triplet absorption decay data were collected using a Laser Flash Reaction Analyzer (LKS.60) from Applied Photophysics. Xanthone as the triplet donor was excited selectively by using a Quantel Nd:YAG-Laser at 354.6 nm with a 4 ns (full width at half maximum; FWHM) pulse of 50 mJ. Peptide concentrations for TTET measurements were in the 20−100 μM range. All measurements were performed in 10 mM potassium phosphate buffer pH 7.0 at 22.5 °C. Transient triplet absorbance of xanthone was measured at 590 nm, and the kinetics were analyzed using ProFit (Quantum Soft, Zürich, Switzerland). Error bars in figures are given by standard deviation obtained from ProFit.

Conductivity Measurements. Ion movement was studied by measuring the electrical conductivity of a 50 mM NaCl solution using a 217 conductometer from Metrohm. All measurements were performed at 22.5 °C.

DLS Measurements. Hydrodynamic radii were measured by dynamic light scattering (for ethylene glycol, glycerol, glucose, sucrose, PEG 400, PEG 600, and PEG 1000) or taken from Krasilnikov et al.[30] (for PEG 1500, PEG 6000 and PEG 20000) and Sauer et al.[7] (Ficoll-70). DLS experiments were carried out on an ALV DLS/SLS-5000 system equipped with a compact goniometer system (ALV, Langen, Germany). All hydrodynamic radii were determined from a concentration dependence and linear extrapolation to zero concentration ($c \rightarrow 0$).

RESULTS AND DISCUSSION

Effect of Solvent Viscosity on Bimolecular TTET from Xanthonic Acid to 1-Naphthylalanine. A model-free interpretation of experiments on the effect of solvent viscosity on loop formation in unfolded polypeptide chains requires a probing reaction that is fully diffusion-controlled, i.e., exhibits a $1/\eta$ viscosity dependence according to eq 2

$$D = \frac{k_B T}{6\pi\eta r_h} \tag{2}$$

where D is the diffusion coefficient and r_h is the hydrodynamic radius. We tested the viscosity dependence of the TTET probing reaction in bimolecular experiments between xanthonic acid (Xan) and 1-naphthylalanine (Nal). The bimolecular rate constant for TTET between xanthonic acid and Nal has a rate constant of $k_T = 3.0 \times 10^9$ M^{-1} s^{-1}, which increases to 4.1×10^9 M^{-1} s^{-1} when the smaller naphthylacetic acid is used as the acceptor.[22,31] These values are in good agreement with the expected rate constants for a diffusion-controlled bimolecular reaction according to Smoluchoswki theory.[32] Determining the rate constant for intermolecular TTET in the presence of various amounts of glycerol (Figure 1) shows that increasing solvent viscosity slows down the

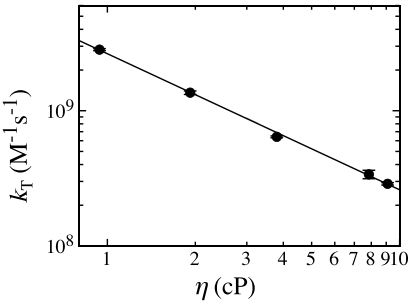

Figure 1. Effect of solvent viscosity on the rate constant for intermolecular TTET between xanthonic acid and naphthylalanine (Nal). Viscosity was modified by adding different concentrations of glycerol to an aqueous solution of 10 mM potassium phosphate at pH 7.0 and 22.5 °C. The bimolecular rate constants at each viscosity were determined in TTET experiments under pseudo-first-order conditions with an excess of Nal.

TTET kinetics and that the bimolecular rate constant is inversely proportional to solvent viscosity ($\alpha = 1.01 \pm 0.02$, see eq 1), as expected for a fully diffusion-controlled reaction (see eq 2). Thus, the TTET process itself does not modulate the viscosity dependence observed for the dynamics of intrachain loop formation described in the following.

Effect of Different Co-Solutes on the Viscosity Dependence of End-to-End Loop Formation in Unfolded Polypeptide Chains. We synthesized different polypeptide chains that do not form stable secondary and/or tertiary structures to study the effect of solvent viscosity on end-to-end loop formation in unfolded peptides and proteins. All chains have the general sequence shown in Figure 2 with Xan attached at the N-terminus and Nal located near the C-terminus. To test for differences in the effect of solvent viscosity on local and long-range loop formation reactions, we investigated the effect of solvent viscosity on loop formation in poly(Gly-Ser) and polySer homopolypeptide chains with different loop sizes. We further measured the dynamics of loop closure in the presence of different viscogenic agents to test whether the viscosity effect depends on the nature of the co-solute. Figure 3 compares TTET kinetics in a $(Gly\text{-}Ser)_{14}$ loop in water at 22.5 °C ($\eta = 0.94$ cP) with the kinetics at $\eta = 2.5$ cP and at $\eta = 10.3$ cP, which was achieved by adding either glycerol or PEG 20000. TTET kinetics were followed by the transient triplet absorbance decay of Xan at 590 nm after laser excitation with a 4 ns pulse at 355 nm. The kinetics can be described by a double exponential function. The major kinetic phase corresponds to loop formation leading to intramolecular TTET between Xan and Nal. A small fraction of triplet states (<10%) decays in a slow reaction with a rate constant that corresponds to the intrinsic triplet lifetime of Xan. This reaction is due to molecules that do not undergo TTET during the donor lifetime, most likely due to formation of oligomers, since its amplitude decreases in good solvents, e.g., in aqueous solutions of urea or GdmCl.[11,22] Figure 3 shows that the presence of either glycerol or PEG 20000 slows down loop formation in the $(Gly\text{-}Ser)_{14}$-peptide compared to water with a stronger effect observed at 10.3 cP compared to 2.5 cP. However, at both viscosities, the magnitude of the effect

https://doi.org/10.1021/acs.jpcb.3c04070
J. Phys. Chem. B 2023, 127, 8095−8105

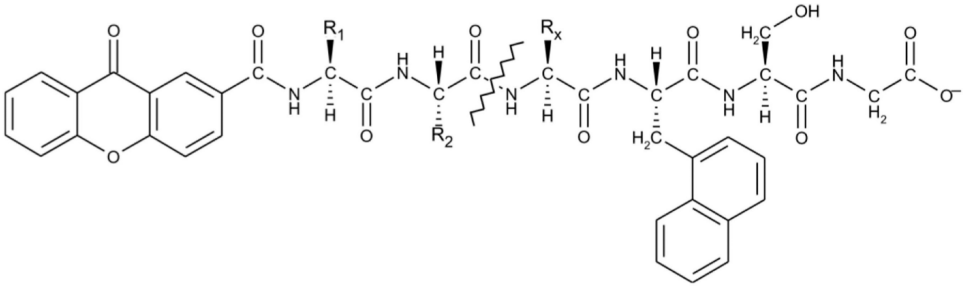

Figure 2. Canonical structure of the polypeptide chains used to study loop formation by intramolecular TTET with Xan attached at the N-terminus and Nal attached near the C-terminus.

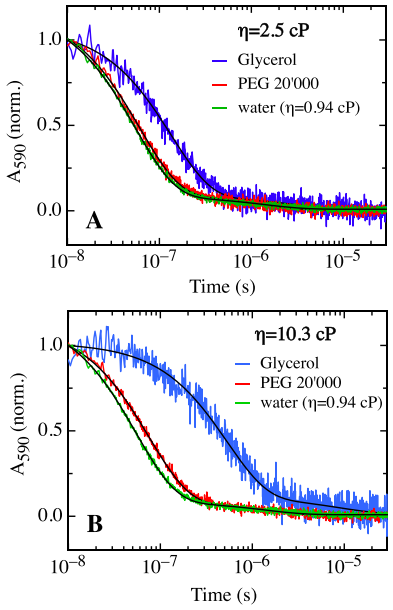

Figure 3. Effect of solvent viscosity on the kinetics of loop formation in a chain with $(Gly\text{-}Ser)_{14}$ between the TTET labels. The effect of a large co-solute (PEG 20000) and of a small co-solute (glycerol) are compared at η = 2.5 cP (A) and η = 10.3 cP (B). Conditions were 10 mM potassium phosphate at pH 7.0 and 22.5 °C. The black lines represent the results from double exponential fits. The fast kinetic phase (>90% amplitude) represents TTET through loop formation with the rate constants shown in Figure 4. The slow kinetic phase (<10% amplitude) has a time constant of about 10 μs, which corresponds to the intrinsic lifetime of the Xan triplet state and is probably due to a small fraction of oligomeric or aggregated peptides.[22]

depends on the nature of the co-solute. The larger PEG 20000 slows down loop formation much less than glycerol. Figure 4 shows the viscosity dependence of the rate constants for formation of the $(Gly\text{-}Ser)_{14}$ loop for several co-solutes with different hydrodynamic radii between 0.18 nm (ethylene glycol) and 5.1 nm (PEG 20000). A fit of eq 1 to the data yields the α-values for loop formation, i.e., the sensitivity of the reaction to solvent viscosity for the different co-solutes (eq 1; Figure 4). The results show that the viscosity effect exerted by a co-solute depends on the hydrodynamic radius of the co-solute. α is as low as 0.1 for large co-solutes and increases with decreasing co-solute size until a limiting value is reached below a critical co-solute size, r_c (Figure 5). Similar results were obtained for $(Gly\text{-}Ser)_n$ loops with n = 1 and 6 and for a Ser_2 loop. In all peptides, increasing solvent viscosity slows down end-to-end loop formation, and in all peptides, the magnitude of the effect depends on co-solute size (Figures 4 and 5). Furthermore, α reaches a limiting value, α_c, below a certain co-solute size, r_c, for all peptides. These results show that the macroscopic solvent viscosity and the microscopic viscosity experienced by the internal dynamics of a polypeptide chain are only identical for small co-solutes below a critical size (r_c). They further indicate that large co-solutes, like large-molecular-weight PEGs and Ficoll-70 (see below), that are typically used to mimic the effect of macromolecular crowding in cells, have very little effect on the internal dynamics in unfolded proteins (α = 0.1−0.2). A similar effect was observed for the rate constant of oxygen escape from the native state of hemerythrin, which is less affected by large co-solutes compared to small co-solutes.[33]

Effect of Chain Length and Amino Acid Sequence on the Viscosity Dependence of End-to-End Loop Formation in Unfolded Polypeptide Chains. Figure 5 shows that the α_c-value for the coupling of solvent motions to chain motions, i.e., the α-value that is observed for loop formation below the critical co-solute size, r_c, depends on loop size and amino acid sequence, which shows that α_c reflects an intrinsic chain property. The effect of loop size on α_c for poly(Gly-Ser) and polyserine chains is displayed in Figure 6A. For poly(Gly-Ser) chains with n > 8 (N > 17), k_c decreases with $1/\eta$ (α_c = 1), indicating that loop closure for long loops is diffusion-controlled and that large-scale polypeptide chain motions are directly coupled to solvent motions. For shorter chains with n < 8 (N < 17), α_c is smaller than 1 and decreases with decreasing loop size, indicating a weaker coupling of solvent motions to chain motions. The lowest value is found for the $(Gly\text{-}Ser)_1$ loop with α_c = 0.75. Similar results were found for stiffer polyserine loops (Figures 5 and 6A) with slightly larger α_c-values for formation of very short loops but a weaker effect of loop size on α_c compared to poly(Gly-Ser) loops (Figure 6A). Due to limitations in peptide synthesis, we were not able to study longer polyserine loops with n > 15. It thus remains unclear whether α_c also reaches a limiting-value of 1 for formation of very long polyserine loops. The different degrees of coupling of solvent motions to chain motions observed for formation of short and long loops are in agreement with conclusions from previous TTET measurement on the effect of loop-length on the rate constant for loop formation, k_c, in unfolded poly(Gly-Ser) chains (Figure 6B). These experiments had shown that k_c scales with loop size ($k_c \sim n^{-1.7 \pm 0.1}$) for long loops with N > 17, as expected from polymer theory for a Gaussian chain with excluded volume effects.[22] This suggested a diffusive search process, which is in agreement with the $1/\eta$ (α_c = 1) viscosity dependence observed for long loops in the present work. Comparison of Figure 6A and B shows that an

https://doi.org/10.1021/acs.jpcb.3c04070
J. Phys. Chem. B 2023, 127, 8095−8105

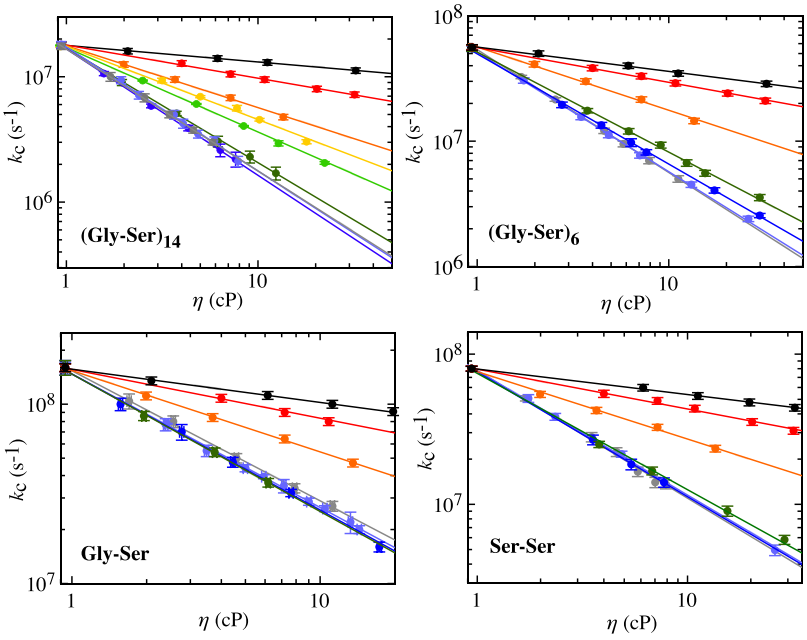

Figure 4. Effect of solvent viscosity on the kinetics of loop formation in different polypeptide chains as indicated in the individual panels. Solvent viscosity was increased by adding different co-solutes: (black circle) PEG 20000, (red circle) PEG 6000, (orange circle) PEG 1500, (yellow circle) PEG 1000, (bright green circle) PEG 600, (dark green circle) sucrose, (bright blue circle) glucose, (light blue circle) glycerol, (gray circle) ethylene glycol. Conditions were 10 mM potassium phosphate at pH 7.0 and 22.5 °C.

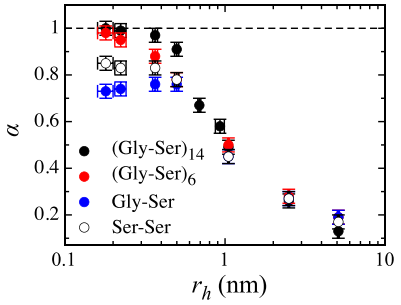

Figure 5. Effect of co-solute size on the sensitivity of loop formation kinetics to solvent viscosity (α) in the different polypeptide chains displayed in Figure 4. The hydrodynamic radius (r_h) of the co-solutes was measured by dynamic light scattering.

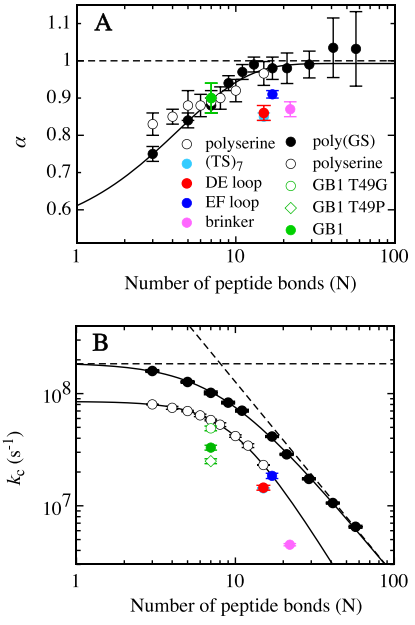

Figure 6. (A) Effect of chain length and amino acid sequence on (A) the α_c-value, i.e., the α-value that is observed for loop formation below a critical co-solute size, and (B) the rate constant for loop formation (k_c). For polyserine with N = 3−12 and poly(Gly-Ser), k_c-values were taken elsewhere.[22]

α_c-value of 1 is observed when the Gaussian chain limit is reached. The rate constant for the closure of short loops, in contrast, becomes virtually independent of loop length (Figure 6B), which shows that different dynamic processes govern local dynamics compared to large-scale motions. Our results show that these local loop formation reactions exhibit a weaker viscosity dependence (α_c < 1), indicating that local chain dynamics exhibit a weaker coupling to solvent motions than large-scale motions. The α_c-values for formation of short loops are in the same range as those reported for local internal dynamics in 1,2-polybutadiene (α = 0.82),[15] polystyrene (α = 0.76),[13] and polyisoprene (α = 0.75)[16] measured by time-resolved optical spectroscopy. Results for the viscosity dependence of large-scale motions in other polymer chains have not been reported up to date, and thus, it remains unclear whether these also exhibit α_c = 1 as observed for long and flexible poly(Gly-Ser) chains.

Correlation between the Critical Co-Solute Size and the Length-Scale of Molecular Motions. Above a critical co-solute size (r_c), the effect of solvent viscosity on loop formation in poly(Gly-Ser) and polyserine chains decreases with increasing size of the co-solute, indicating that the chain motions do not feel the macroscopic solvent viscosity (Figure 4). Similar effects were observed for free diffusion of T_2O molecules in water in the presence of co-solutes of different sizes[34] and for the effect of co-solute size on translational diffusion coefficients of various native proteins, polymers, and fluorescent dyes.[35] From these results, it was proposed that the

https://doi.org/10.1021/acs.jpcb.3c04070
J. Phys. Chem. B 2023, 127, 8095−8105

microviscosity experienced by a freely diffusing molecule matches macroviscosity only when the co-solute is smaller than the moving particle. A correlation between the size of a moving particle and r_c implies a correlation between the length scale of a moving chain segment in an unfolded chain, i.e., the persistence length of a chain, and r_c. Thus, it should be possible to gain information on the persistence length by determining r_c. This requires, however, knowledge of the relationship between r_c and the size of the moving object. We therefore studied the effect of different co-solutes on the viscosity dependence of free diffusion for Na^+ and Cl^- ions and for the triplet labels Xan and Nal to determine r_c for moving particles of different sizes.

The effect of solvent viscosity on the diffusion coefficients of Na^+ and Cl^- was determined by measuring electrical conductivity of a 50 mM sodium chloride solution. The measured conductivity, κ, can be described by the Nernst–Einstein equation

$$\kappa = \frac{z^2F^2}{RT}[D_+ + D_-] \quad (3)$$

where z is the charge of the ion, F is Faraday's constant, R is the gas constant, and T is the absolute temperature in K. $D_{+/-}$ are the diffusion coefficients of the cation and the anion, respectively, which change with solvent viscosity according to eq 2. Since all co-solutes used in this study are uncharged, they should not induce additional effects on conductivity. Figure 7A,C shows that the α-value for the motion of Na^+ and Cl^- in solution does not reach a limiting value even for the smallest co-solutes, but α comes close to 1 for urea (α = 0.98). Although we do not exactly know the Stokes radii of the ions including their hydration shells, this result suggests that the co-solute does not have to be much smaller than the moving particle to exert the full viscosity effect on the moving particle. The triplet probes Xan and Nal are both considerably larger than Na^+ and Cl^- and larger than the smallest co-solutes used in our study. Figure 7B shows the effect of increasing solvent viscosity on the rate constant for bimolecular TTET kinetics between Xan and Nal (k_T). As for NaCl, the viscosity effect exerted by the co-solutes depends on the size of the co-solutes. Large co-solutes have very little effect on k_T with an α-value of 0.1 for PEG 20000. However, in contrast to the diffusion of NaCl, the rate constant reaches a limiting α-value of 1 for co-solutes below a r_h of 0.5 nm (d_h = 1.0) nm (Figure 7C). This value is in the same range as the size of the triplet labels, which shows that the microviscosity experienced by a moving particle matches the macroviscosity of the solution when the co-solute is of the same size or smaller than the moving particle. This finding is in agreement with the results on translational diffusion of three globular proteins under self-crowding conditions, which all showed a $1/\eta$ viscosity dependence,[36] whereas diffusion coefficients of proteins in the presence of very large crowders show $\alpha < 1$.[37,38] Also, results from the diffusion of different size fluorescent probes probed by FCS suggested that microviscosity matches macroviscosity when the size of the co-solute is similar or smaller than that of the diffusing particle.[39]

If the critical co-solute size, r_c, below which microviscosity is identical to macroviscosity, reflects the dimensions of the moving chain segments, then r_c should depend on chain stiffness for large-scale chain motions and thus on the persistence length of the chain. As shown above, the $(Gly\text{-}Ser)_{14}$ loop can be approximated by a flexible Gaussian chain

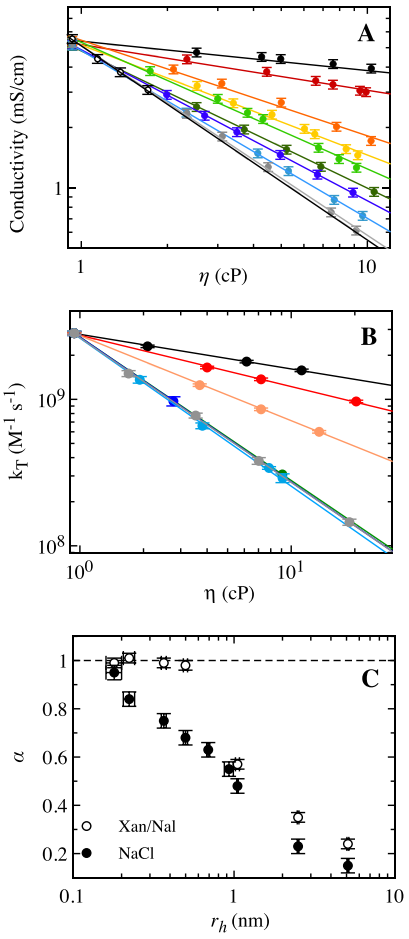

Figure 7. Effect of solvent viscosity on conductivity of (A) a 50 mM NaCl solution and (B) the rate constant for intermolecular TTET between Xan and Nal. Solvent viscosity was increased by adding different co-solutes: (black circle) PEG 20000, (red circle) PEG 6000, (orange circle) PEG 1500, (yellow circle) PEG 1000, (bright green circle) PEG 600, (dark green circle) sucrose, (bright blue circle) glucose, (light blue circle) glycerol, (gray circle) ethylene glycol, and (unshaded circle) urea. Experiments were carried out in water at 22.5 °C. Panel (C) shows the effect of co-solute size on the sensitivity (α) of NaCl mobility and intermolecular TTET between Xan and Nal.

with purely diffusive motions for loop formation. This reaction shows an α_c-value of 1, which is reached between the co-solutes glycerol and glucose (Figures 4 and 5) with hydrodynamic radii of 0.22 and 0.37 nm, respectively. This suggests that below a co-solute diameter ($d_c = 2 \cdot r_c$) of around 0.5–0.7 nm the peptide motions feel the full solvent viscosity. Comparing this limiting co-solute size to the length of a peptide bond (0.35 nm) gives a limiting co-solute size that corresponds to about 2 peptide bonds, which matches the persistence length expected for poly(Gly-Ser) chains.[40] To further test this model, we determined r_c for end-to-end loop formation in a stiffer $(Thr\text{-}Ser)_7$ chain, which is expected to have a similar end-to-end distance as a $(Gly\text{-}Ser)_{14}$ chain but a larger persistence length.[40,41] Due to the lower solubility of the $(Thr\text{-}Ser)_7$ peptide, two additional arginine residues were introduced at the C-terminal end. A corresponding $(Gly\text{-}Ser)_{14}$ chain with two additional arginine residues at the C-terminus was synthesized for comparison and showed a slightly decreased rate constant for loop formation, as expected for end-to-end vs interior loop formation.[42] However, the

https://doi.org/10.1021/acs.jpcb.3c04070
J. Phys. Chem. B 2023, 127, 8095–8105

additional C-terminal amino acids affect neither the critical co-solute size nor the limiting α-value of $\alpha_c = 1$ in the $(Gly\text{-}Ser)_{14}$ peptide (Figure 8). The viscosity dependence of loop formation in the $(Thr\text{-}Ser)_7$ peptide measured in the presence of different co-solutes shows a limiting α_c value of 0.85 for small co-solutes (Figure 8). This limit is reached between sucrose and PEG 400 with hydrodynamic radii of 0.50 nm (d_h = 1.00 nm) and 0.58 nm (d_h = 1.16 nm), respectively, corresponding to the length of about three peptide bonds. This value is larger compared to the limiting size for $(Gly\text{-}Ser)_{14}$; it is, however, shorter than the persistence length in the range of five to seven peptide bonds predicted for the poly(Thr-Ser) chain.[40,41] However, the effect of peptide solvent interactions and intramolecular hydrogen bond formation may reduce the persistence length in real polypeptide chains in solution.

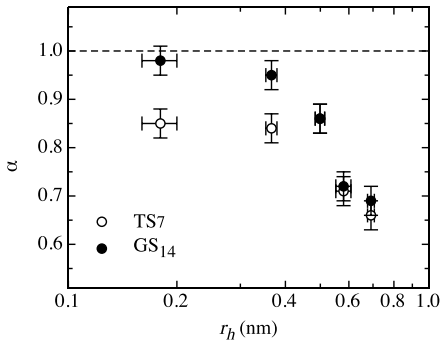

Figure 8. Effect of co-solute size on the sensitivity of loop formation kinetics to solvent viscosity (α) in a flexible $(Gly\text{-}Ser)_{14}$ and a stiffer polypeptide chain $(Thr\text{-}Ser)_7$. Conditions were 10 mM potassium phosphate at pH 7.0 and 22.5 °C.

Effect of Solvent Viscosity on the Dynamics of Formation of Natural Protein Loops. To compare the effect of solvent viscosity on the dynamics of loop formation in homopolypeptide chains to the effect on naturally occurring protein loops with additional steric effects and intramolecular interactions introduced by side chains, we investigated several loop fragments from IDPs. Two loops were derived from carp muscle β-parvalbumin, which is unfolded in the absence of Ca^{2+}. Another fragment represents a loop from the DNA-binding domain of the brinker protein, which is highly positively charged and unfolded in the absence of DNA. In addition, we investigated a short loop from the β-hairpin 1 of protein G (GB1 hairpin). In all cases, two aromatic residues were replaced by the triplet donor and acceptor groups (Figure 9). The parvalbumin DE-loop comprises residues Phe70 to Phe85 of parvalbumin and connects helices D and E by bringing the two phenylalanine residues into van der Waals contact in the native state (Figure 9). We synthesized a 16 amino acid peptide that corresponds to the parvalbumin DE-loop and replaced Phe70 by Xan and Phe85 by Nal (Figure 9). Accordingly, peptides comprising residues F85 to F102 of parvalbumin (EF-loop), residues C24 to W45 of the brinker protein and residues Y45 to F52 of the protein G β-hairpin were synthesized and the N- and C-terminal aromatic residues replaced by Xan and Nal, respectively. CD measurements showed that all loop fragments labeled with the triplet probes are unfolded (Figure S1). TTET kinetics revealed significantly slower rate constants for loop formation for the DE-loop, the brinker fragment, and the GB1 fragment compared to poly(Gly-Ser) and polyserine loops of the same length (Figure 6B), which may in part be explained by the presence of branched side-chains, which were shown to slightly slow down local loop formation.[22] However, contributions from intramolecular side-chain interactions that are absent in polyserine

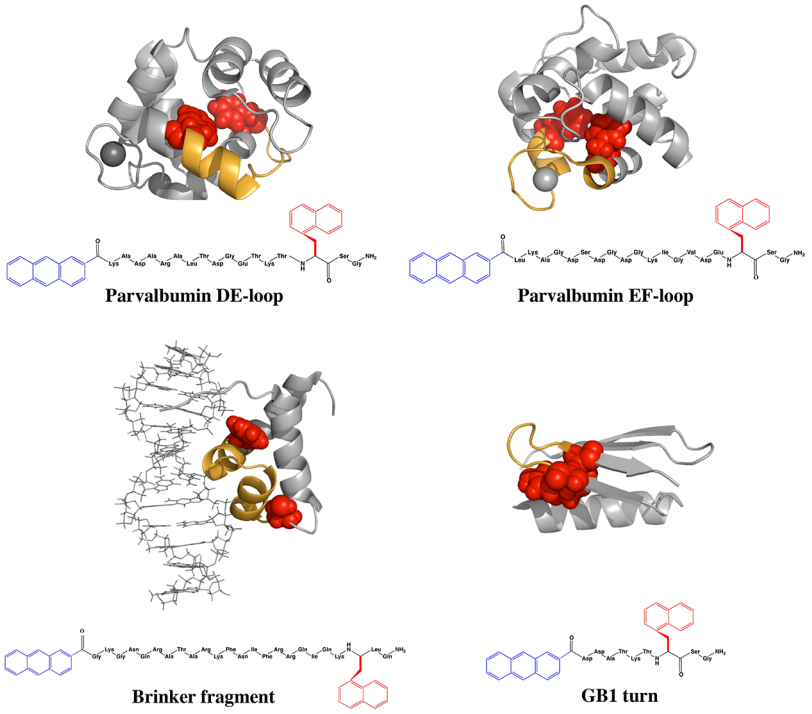

Figure 9. Structures in the native proteins and sequences of the fragments from parvalbumin, the brinker domain, and the GB1 hairpin. The investigated sequences are shown in orange, and the amino acids replaced by Xan/Nal are shown in red.

https://doi.org/10.1021/acs.jpcb.3c04070
J. Phys. Chem. B 2023, 127, 8095−8105

chains may also contribute to the slower dynamics. The EF-loop forms faster than the other natural loops of similar size and shows a similar rate constant for loop formation as expected from the extrapolation of the polyserine data (Figure 6B). This faster loop formation is probably due to the presence of four glycine residues in the EF loop (Figure 9), which accounts for 25% of the loop residues and increases chain flexibility and dynamics.

Figure 10A displays TTET measurements on dynamics of the DE-loop in the presence of different co-solutes. The DE-sequence lead to a weaker coupling of solvent motions to chain dynamics. The limiting α_c-value of 0.86 ± 0.03 for the parvalbumin DE-loop is reached around d_h = 0.8−0.9 nm (Figure 10), which is slightly smaller than d_h for the (Thr-Ser)$_{14}$ chain (Figure 8). This lower value is likely due to the glycine residue at position 10 of the DE-loop, which decreases chain stiffness and thus also the persistence length.

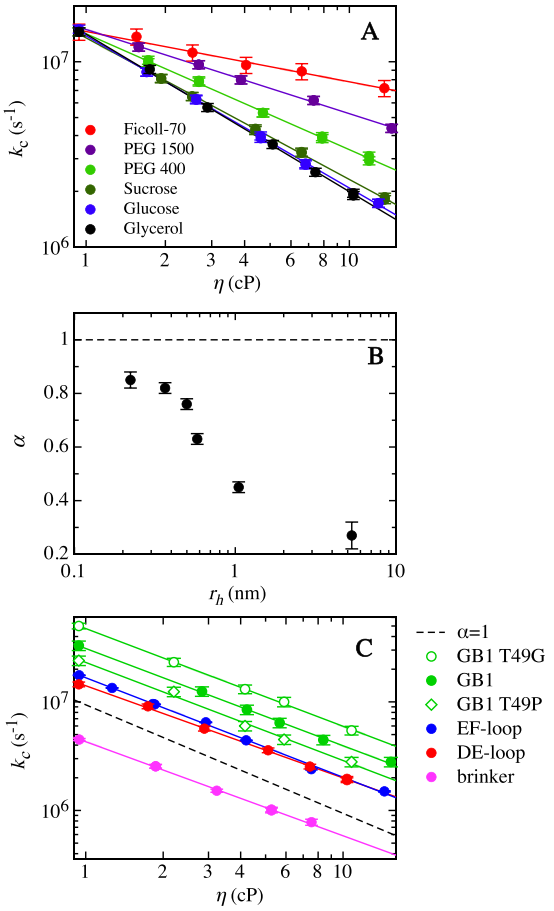

Figure 10. Effect of solvent viscosity on the kinetics of loop formation in loops from proteins in 10 mM potassium phosphate at pH 7.0 and 22.5 °C. (A) Effect of solvent viscosity on k_c for the parvalbumin DE-loop. (B) Effect of co-solute size on the sensitivity of loop formation kinetics to solvent viscosity (α) in the parvalbumin DE-loop. (C) Comparison of the effect of solvent viscosity on k_c for the different natural loop and turn sequences shown in Figure 9. Solvent viscosity was modulated by addition of glycerol.

loop shows a similar behavior to the poly(Gly-Ser) and polyserine loops with a weaker viscosity dependence for larger co-solutes and a limiting α_c-value that is reached below a critical co-solute size (Figure 10A,B). However, the α_c-value is significantly smaller (0.86) than for a poly(Gly-Ser) loop with the same number of amino acids (α = 0.99). It is even smaller than the α_c-value for shorter polyserine loops (Figure 6A), indicating a weaker coupling of chain dynamics to solvent motions in the DE-loop compared to both model homo-polypeptide loops (Figure 6A). This low α_c-value suggests that additional intramolecular side-chain interactions and/or steric effects of the bulkier and branched side chains in the natural

A similar viscosity dependence of k_c as seen for the parvalbumin DE-loop is observed for the other natural loop fragments with α_c-values of α_c = 0.90 ± 0.04 for the GB1turn, α_c = 0.91 ± 0.03 for the EF-loop, and α_c = 0.87 ± 0.03 for the brinker fragment (Figures 10C and 6A), which shows that the viscosity dependence of loop formation in natural sequences is only very little affected by loop length and amino acid sequence. For natural loops, both local and long-range dynamics are not fully coupled to solvent dynamics. The slightly larger value of the EF-loop compared to the DE loop and the brinker fragment suggests that increased chain flexibility introduced by glycine residues increases the α_c-value. Interestingly, the α_c-values for the short GB1 hairpin loop (α_c = 0.90 ± 0.04) and of poly(Gly-Ser) and polyserine loops of the same length, α_c = 0.88 ± 0.02 and 0.89 ± 0.03, respectively, are identical within error, which indicates that the viscosity dependence of local chain dynamics is independent of the amino acid sequence, even when the chains are very flexible. To further test this finding, we replaced the Thr49 of the GB1 hairpin, which is located in the turn region, by Gly and Pro and measured the resulting effect on the rate constant for loop formation and its viscosity dependence. Since glycine and proline residues are energetically favorable in β-turns like the turn region of the GB1 hairpin, these replacements further enabled us to test whether Pro and Gly also favor the dynamics of β-turn formation. As expected, the more flexible Gly residue leads to faster loop formation whereas the stiffer Pro residue has the opposite effect (Figure 6B). However, both loop variants show essentially the same viscosity dependence for loop closure as the wild-type loop (α_c = 0.90 ± 0.04 for all three loops; Figure 6A), which supports the finding that chain stiffness has little effect on the viscosity dependence of local chain dynamics.

CONCLUSIONS

The aim of this work is to elucidate the effect of solvent viscosity on local and large-scale conformational dynamics in unfolded proteins and peptides in order to determine the extent of solvent coupling for motions over different length scales. We tested the extent of coupling of solvent viscosity to chain motions in various unfolded polypeptide chains by measuring the effect of different co-solutes on the dynamics of intrachain loop formation. The results reveal several factors that reduce the coupling of solvent motions to chain motions and thus yield a fractional power law relationship between the rate constant for loop formation and solvent viscosity (α < 1 in eq 1). In fact, a $1/\eta$ correlation between loop formation dynamics and solvent viscosity is a rather special case. It is only observed for formation of long loops (>17 amino acids) in very flexible poly(Gly-Ser) chains and only in the presence of small co-solutes. Loop formation in all other investigated chains shows α < 1, even in the presence of small co-solutes. Several previous studies have assumed that internal motions in unfolded peptides and proteins are fully coupled to solvent viscosity, i.e., show a $1/\eta$ viscosity dependence as observed for free diffusion.[7−9] A weaker viscosity dependence of loop

https://doi.org/10.1021/acs.jpcb.3c04070
J. Phys. Chem. B 2023, 127, 8095−8105

formation has major effects on the calculated intrachain diffusion times derived from experimental systems that are not diffusion controlled.

The size of the co-solute used to modulate viscosity influences the sensitivity of chain dynamics to macroscopic solvent viscosity independent of loop length and amino acid sequence. For all polypeptide chains characterized in this study, only small co-solutes below a critical hydrodynamic radius (r_c) exert the maximum viscosity effect. Below this r_c, the α-value is constant and reflects the true extent of solvent coupling to chain motions. Above r_c, the effect of solvent viscosity on loop formation dynamics decreases with increasing co-solute size, indicating that the macroviscosity of the solvent does not match the microviscosity experienced by the chain motions for larger co-solutes. A possible explanation for this effect is the presence of water cavities in solutions of large co-solutes that have similar properties as bulk water (caging) and thus form regions of low microviscosity experienced by the peptides.[43,44] Alternatively, large co-solutes may interact less strongly with the polypeptide backbone and thus have less effect on internal chain motions. The results on the effect of co-solute size on free diffusion of Na^+/Cl^- and of Xan and Nal (Figure 7) revealed that the microviscosity matches macroviscosity when the co-solute is of similar size or smaller than the moving particle. Applied to chain motions, this observation suggests that the critical co-solute size depends on the size of the moving chain segments and thus reflects the persistence length of a chain. This interpretation is supported by the smaller r_c-value observed for loop formation of the more flexible $(Gly\text{-}Ser)_{14}$ loop compared to the stiffer $(Thr\text{-}Ser)_7$ and parvalbumin DE-loop (Figures 8 and 9).

The weak viscosity effect of large co-solutes on the dynamics of loop formation shows that macromolecular crowders that are present in living cells have very little effect on the internal dynamics in unfolded proteins. The α-values for large co-solutes like Ficoll and PEG 20000, which are commonly used to mimic macromolecular crowding in cells, are between 0.1 and 0.2 (Figures 4 and 5). These low α-values result in only minor effects on both local and large-scale dynamics of loop formation inside cells where viscosities of 2−4 cP were measured[35] and even at very high macroscopic solvent viscosities. Our findings also explain results from recent experiments that showed only little differences between *in vivo* folding rate constants and *in vitro* values measured at the solvent viscosity of water.[45] In addition, the minor effect of large co-solutes on the diffusion coefficient for free diffusion of small molecules in solutions (Figure 7) suggests that also bimolecular reactions in cells are only little affected by macromolecular crowding, which is in agreement with several experimental studies that showed only little differences between intermolecular diffusion processes in cells and in water.[46] Our results are further in agreement with the finding that association rate constants for protein−protein interactions are less influenced by large co-solutes than by small co-solutes.[47−50]

An alternative model for a reduced sensitivity of dynamic processes to solvent viscosity in the presence of large macromolecular crowding agents assumes that crowding decreases the free space available for the moving particles and thus leads to acceleration of bimolecular reactions and to chain compaction in unfolded proteins. This compaction reduces the diffusion distances for intrachain dynamics during folding.[51,52] Such a model seems unlikely to explain our data on the dynamics of loop formation, since the same co-solutes give nearly identical α-values for all chains, independent of loop length and amino acid sequence and also for free diffusion of molecules (Figures 5 and 7). Furthermore, small co-solutes like glycerol, sucrose, and glucose have a similar excluded volume effect on unfolded polypeptide chains as large co-solutes but show $\alpha = 1$ for chain dynamics and bimolecular TTET.

Besides the general effect of large co-solutes, also intrinsic chain properties lead to reduced α-values even for co-solutes smaller than r_c. Comparison of α_c-values for formation of long and short poly(Gly-Ser) loops reveals different degrees of solvent coupling to local and large-scale chain motions even in very flexible chains. Formation of short poly(Gly-Ser) loops exhibits α_c-values as low as 0.75, whereas α_c-values of 1 are observed for long loops with $N > 17$, which can be approximated by a Gaussian chain.[22] This result supports our previous finding that local chain motions are limited by different processes than large-scale motions.[22] Large-scale motions of a flexible polypeptide chain are fully coupled to solvent motions and are thus compatible with a purely diffusive process, whereas local motions show weaker coupling to bulk solvent. The weak coupling of local motions to solvent motions may have different origins. As observed for the dynamics of native proteins, large-scale and local chain motions may be coupled to different solvent modes. This would indicate that large-scale motions are coupled to motions of the bulk solvent (α-motions) and thus show a $1/\eta$ viscosity dependence, whereas local motions may contain contributions from solvation shell dynamics, which were observed to be independent of solvent viscosity ($\alpha = 0$)[5] in native proteins. However, only little information is available on the dynamics of solvation shell water in unfolded proteins. Another possible origin of α_c-values <1 is memory friction. Grote−Hynes theory predicts $\alpha_c < 1$ for barrier crossing processes when the time scale of barrier crossing is similar to the time scale of solvent motions.[53] This would suggest that local motions that lead to loop formation, which mainly require rotation around a few backbone bonds, are on the same time scale as solvent motions and thus lead to memory friction, i.e., reduce the sensitivity of the reaction to solvent viscosity. A similar explanation was given for the effect of solvent viscosity on the rate constants of photoisomerization of diphenylbutadiene and the dye molecule DODCI and for local chain dynamics in various synthetic linear polymers, which all showed α-values <1.[13−18,54,55] These reduced viscosity dependencies were ascribed to the presence of barriers for bond rotations and were suggested to be in accordance with Grote−Hynes theory of memory friction.[13−18,54−56] Based on MD simulations, Best and co-workers also reported that barriers for local bond rotations in short peptides lead to a reduced sensitivity of the rotations to solvent viscosity.[19] Although dynamics of loop formation are more complex than single bond rotations, coupling multiple barriers for bond rotations during loop formation may result in a similar effect on the viscosity dependence. A reduced viscosity dependence of chain motions due to intrinsic barriers can further explain the reduced effect of solvent viscosity on large-scale peptide dynamics observed for the formation of large loops in the longer polyserine chains, in the $(Thr\text{-}Ser)_7$ loop, and in the long natural sequences compared to poly(Gly-Ser) loops. Increased chain stiffness, steric effects induced by branched side chains, and side-chain interactions create additional barriers for chain motions, which reduces the

https://doi.org/10.1021/acs.jpcb.3c04070
J. Phys. Chem. B 2023, 127, 8095−8105

sensitivity to solvent viscosity even for long chains. The accompanying paper addresses the activation parameters for loop formation in order to characterize the barriers for the different types of chain motions and to elucidate the molecular origin of the observed differences in the coupling of solvent motions to chain dynamics.

■ ASSOCIATED CONTENT

Supporting Information

The Supporting Information is available free of charge at https://pubs.acs.org/doi/10.1021/acs.jpcb.3c04070.

CD spectra of the IDP peptides and GB1 turn peptide (PDF)

■ AUTHOR INFORMATION

Corresponding Author

Thomas Kiefhaber − *Abteilung Proteinbiochemie, Institut für Biochemie und Biotechnologie, Martin-Luther-Universität Halle-Wittenberg, Halle (Saale) 06120, Germany;* orcid.org/0009-0009-2429-764X; Phone: +49 345 552 4860; Email: t.kiefhaber@biochemtech.uni-halle.de

Authors

Karin Stecher − *Chemistry Department, Technische Universität München, Garching D-85747, Germany*

Florian Krieger − *Biozentrum der Universität Basel, Basel CH-4056, Switzerland*

Michael Schleeger − *Abteilung Proteinbiochemie, Institut für Biochemie und Biotechnologie, Martin-Luther-Universität Halle-Wittenberg, Halle (Saale) 06120, Germany;* orcid.org/0000-0003-2388-9087

Complete contact information is available at: https://pubs.acs.org/10.1021/acs.jpcb.3c04070

Author Contributions

#K.S. and F.K. contributed equally.

Notes

The authors declare no competing financial interest.

■ ACKNOWLEDGMENTS

This work was supported by the Deutsche Forschungsgemeinschaft (SFB 863-A6, SFB/TRR 102-A10, INST 271/359-1 FUGG, and INST 271/345-1 FUGG).

■ REFERENCES

(1) Beece, D.; Eisenstein, L.; Frauenfelder, H.; Good, D.; Marden, M. C.; Reinisch, L.; Reynolds, A. H.; Sorensen, L. B.; Yue, K. T. Solvent Viscosity and Protein Dynamics. *Biochemistry* **1980**, *19*, 5147−5157.

(2) Fenimore, P. W.; Frauenfelder, H.; McMahon, B. H.; Parak, F. G. Slaving: Solvent fluctuations dominate protein dynamics and functions. *Proc. Natl. Acad. Sci. U. S. A.* **2002**, *99*, 16047−16051.

(3) Frauenfelder, H.; Chen, G.; Berendzen, J.; Fenimore, P. W.; Jansson, H.; McMahon, B. H.; Stroe, I. Z.; Swenson, J.; Young, R. D. A unified model for protein dynamics. *Proc. Natl. Acad. Sci. U. S. A.* **2009**, *106*, 5129−5134.

(4) Doster, W. Viscosity Scaling and Protein Dynamics. *Biophys. Chem.* **1983**, *17*, 97−103.

(5) Fenimore, P. W.; Frauenfelder, H.; McMahon, B. H.; Young, R. D. Bulk-solvent and hydration-shell fluctuations, similar to alpha- and beta-fluctuations in glasses, control protein motions and functions. *Proc. Natl. Acad. Sci. U. S. A.* **2004**, *101*, 14408−14413.

(6) Kramers, H. A. Brownian motion in a field of force and the diffusion model of chemical reactions. *Physica* **1940**, *7*, 284−304.

(7) Neuweiler, H.; Löllmann, M.; Doose, S.; Sauer, M. Dynamics of unfolded polypeptide chains in crowded environment studied by fluorescence correlation spectroscopy. *J. Mol. Biol.* **2007**, *365*, 856−869.

(8) Lapidus, L. J.; Steinbach, P. J.; Eaton, W. A.; Szabo, A.; Hofrichter, J. Effects of chain stiffness on the dynamics of loop formation in polypeptides. Appendix: Testing a 1-diensional diffusion model for peptide dynamics. *J. Phys. Chem. B* **2002**, *106*, 11628−11640.

(9) Acharya, S.; Srivastava, K. R.; Nagarajan, S.; Lapidus, L. J. Monomer dynamics of Alzheimer peptides and kinetic control of early aggregation in Alzheimer's disease. *ChemPhysChem* **2016**, *17*, 3470−3479.

(10) Sorrano, A.; Buchli, B.; Nettels, D.; Cheng, R. R.; Müller-Späth, S.; Pfeil, S. H.; Hoffmann, A.; Lipman, E. A.; Makarov, D. E.; Schuler, B. Quantifying internal friction in unfolded and intrinsically disordered proteins with single-molecule spectroscopy. *Proc. Natl. Acad. Sci. U. S. A.* **2012**, *109*, 17800−17806.

(11) Möglich, A.; Krieger, F.; Kiefhaber, T. Molecular basis for the effect of urea and guanidinium chloride on the dynamics of unfolded polypeptide chains. *J. Mol. Biol.* **2005**, *345*, 153−162.

(12) Krieger, F.; Möglich, A.; Kiefhaber, T. Effect of proline and glycine residues on dynamics and barriers of loop formation in polypeptide chains. *J. Am. Chem. Soc.* **2005**, *127*, 3346−3352.

(13) Zhu, W.; Ediger, M. D. Viscosity Dependence of Polystyrene Local Dynamics in Dilute Solutions. *Macromolecules* **1997**, *30*, 1205−1210.

(14) Zhu, W.; Gisser, D. J.; Ediger, M. D. C-13 Nmr Measurements of Polybutadiene Local Dynamics in Dilute-Solution - Further Evidence for Non-Kramers Behavior. *J. Pol. Sci., Part B: Polym. Phys.* **1994**, *32*, 2251−2262.

(15) Adams, S.; Adolf, D. B. Viscosity dependence of the local segmental dynamics of anthracene-labeled 1,2-polybutadiene in dilute solutions. *Macromolecules* **1998**, *31*, 5794−5799.

(16) Adolf, D. B.; Ediger, M. D.; Kitano, T.; Ito, T. Viscosity dependence of the local segmental dynamics of antracene-labeled polyisoprene in dilute solutions. *Macromolecules* **1992**, *25*, 867−872.

(17) Zhu, W.; Ediger, M. D. Deuterium NMR characterization of 1,2-polybutadiene local dynamics in dilute solutions. *Macromolecules* **1995**, *28*, 7549−7557.

(18) Glowinkowski, S.; Gisser, D. J.; Ediger, M. D. Carbon-13 nuclear magnetic resonance measurements of local segmental dynamics of polyisoprene in dilute solution: nonlinear viscosity dependence. *Macromolecules* **1990**, *23*, 3520−3530.

(19) Zheng, W.; de Sancho, D.; Best, R. B. Modulation of folding internal friction by local and global barrier heights. *J. Phys. Chem. Lett.* **2016**, *7*, 1028−1034.

(20) Lee, Y. R.; Kwon, S.; Sung, B. J. The non-classical kinetics and the mutual information of polymer loop formation. *J. Chem. Phys.* **2020**, *152*, No. 184905.

(21) Bieri, O.; Wirz, J.; Hellrung, B.; Schutkowski, M.; Drewello, M.; Kiefhaber, T. The speed limit for protein folding measured by triplet-triplet energy transfer. *Proc. Natl. Acad. Sci. U. S. A.* **1999**, *96*, 9597−9601.

(22) Krieger, F.; Fierz, B.; Bieri, O.; Drewello, M.; Kiefhaber, T. Dynamics of unfolded polypeptide chains as model for the earliest steps in protein folding. *J. Mol. Biol.* **2003**, *332*, 265−274.

(23) Fierz, B.; Satzger, H.; Root, C.; Gilch, P.; Zinth, W.; Kiefhaber, T. Loop formation in unfolded polypeptide chains on the picoseconds to microseconds time scale. *Proc. Natl. Acad. Sci. U. S. A.* **2007**, *104*, 2163−2168.

(24) Krieger, F.; Fierz, B.; Axthelm, F.; Joder, K.; Meyer, D.; Kiefhaber, T. Intrachain diffusion in a protein loop fragment from carp parvalbumin. *Chem. Phys.* **2004**, *307*, 209−215.

(25) Möglich, A.; Joder, K.; Kiefhaber, T. End-to-end distance distributions and intrachain diffusion constants in unfolded

polypeptide chains indicate intramolecular hydrogen bond formation. *Proc. Natl. Acad. Sci. U. S. A.* **2006**, *103*, 12394−12399.
(26) Heinz, B.; Schmidt, B.; Root, C.; Satzger, H.; Milota, F.; Fierz, B.; Kiefhaber, T.; Zinth, W.; Gilch, P. On the unusual fluorescence properties of xanthone in water. *Phys. Chem. Chem. Phys.* **2006**, *8*, 3432−3439.
(27) Satzger, H.; Schmidt, B.; Root, C.; Zinth, W.; Fierz, B.; Krieger, F.; Kiefhaber, T.; Gilch, P. Ultrafast quenching of the xanthone triplet by energy transfer: new insight into the intersystem crossing kinetics. *J. Phys. Chem. A* **2004**, *108*, 10072−10079.
(28) Graham, R.; Lewis, J. R. Synthesis of 9-oxoxanthen-2-carboxylic acids. *J. Chem. Soc. Perkin Trans. 1* **1978**, 876−881.
(29) Stewart, C. J.; Olgenblum, G. I.; Propst, A.; Harries, D.; Pielak, G. J. Resolving the enthalpy of protein stabilization by macromolecular crowding. *Protein Sci.* **2023**, *32*, No. e4573.
(30) Krasilnikov, O. V.; Sabirov, R. Z.; Ternovsky, V. I.; Merzliak, V. I.; Muratkhodjaev, J. N. A simple method for the determination of the pore radius of ion channels in planar lipid bilayers. *FEMS Microbiol. Lett.* **1992**, *105*, 93−100.
(31) Fierz, B.; Kiefhaber, T., Dynamics of unfolded polypeptide chains. In *Protein Folding Handbook*, Buchner, J.; Kiefhaber, T., Eds. WILEY-VCH: Weinheim, 2005; pp. 805−851.
(32) von Smoluchowski, M. V. Versuch einer mathematischen Theorie der Koagulationskinetik kolloider Lösung. *Z. Phys. Chem.* **1917**, *92*, 129−168.
(33) Yedgar, S.; Tetreau, C.; Gavish, B.; Lavalette, D. Viscosity dependence of O2 escape from respiratory proteins as a function of cosolvent molecular weight. *Biophys. J.* **1995**, *68*, 665−670.
(34) Barshtein, G.; Almagor, A.; Yedgar, S.; Gavish, B. Inhomogeneity of viscous aqueous solutions. *Phys. Rev. E* **1995**, *52*, 555−557.
(35) Kalwarczyk, T.; Ziebacz, N.; Bielejewska, A.; Zaboklicka, E.; Koynov, K.; Szymanski, J.; Wilk, A.; Patkowski, A.; Gapinski, J.; Butt, H.-J.; et al. Comparative Analysis of Viscosity of Complex Liquids and Cytoplasm of Mammalian Cells at the Nanoscale. *Nano Lett.* **2011**, *11*, 2157−2163.
(36) Roos, M.; Ott, M.; Hofmann, M.; Link, S.; Rössler, E.; Balbach, J.; Krushelnitsky, A.; Saalwächter, K. Coupling and decoupling of rotational and translational diffusion of proteins under crowding conditions. *J. Am. Chem. Soc.* **2016**, *138*, 10365−10372.
(37) Phillies, G. D. J.; Ullman, G. S.; Ullman, K.; Lin, T.-H. Phenomenological scaling laws for "semidilute" macromolecule solutions from light scattering by optical probe particles. *J. Chem. Phys.* **1985**, *82*, 5424−5426.
(38) Banks, D. S.; Fradin, C. Anomalous diffusin of proteins due to molecular crowding. *Biophys. J.* **2005**, *89*, 2960−2971.
(39) Holyst, R.; Bielejewska, A.; Szymanski, J.; Wilk, A.; Patkowski, A.; Gapinski, J.; Zywocinski, A.; Kalwarczyk, T.; Kalwarczyk, E.; et al. Scaling form of viscosity at all length-scales in poly(ethylene glycol) solutions studied by fluorescence correlation spectroscopy and capillary electrophoresis. *Phys. Chem. Chem. Phys.* **2009**, *11*, 9025−9032.
(40) Miller, W. G.; Brant, D. A.; Flory, P. J. Random coil configurations of polypeptide chains. *J. Mol. Biol.* **1967**, *23*, 67−80.
(41) Brant, D. A.; Flory, P. J. The configuration of random polypeptide chains. *II. Theory. J. Am. Chem. Soc.* **1965**, *87*, 2791−2800.
(42) Fierz, B.; Kiefhaber, T. End-to-end vs interior loop formation kinetics in unfolded polypeptide chains. *J. Am. Chem. Soc.* **2007**, *129*, 672−679.
(43) Shin, J.; Cherstvy, A. G.; Metzler, R. Polymer Looping Is Controlled by Macromolecular Crowding, Spatial Confinement, and Chain Stiffness. *ACS Macro Lett.* **2015**, *4*, 202−206.
(44) Shin, J.; Cherstvy, A. G.; Metzler, R. Kinetics of polymer looping with macromolecular crowding: effects of volume fraction and crowder size. *Soft Matter* **2015**, *11*, 472−488.
(45) Ebbinghaus, S.; Dhar, A.; Douglas McDonald, D.; Gruebele, M. Protein folding stability and dynamics imaged in a living cell. *Nat. Methods* **2010**, *7*, 319−323.
(46) Dix, J. A.; Verkman, A. S. Crowding effects on diffusion in solution and cells. *Annu. Rev. Biophys.* **2008**, *37*, 247−263.
(47) Teschner, W.; Rudolph, R.; Garel, J.-R. Intermediates in the folding pathway of octopine dehydrogenese from pecten jocobaeus. *Biochemistry* **1987**, *26*, 2791−2796.
(48) Ladurner, A. G.; Fersht, A. R. Upper limit of the time scale for diffusion ande chain collapse in chymotrypsin inhibitor 2. *Nat. Struct. Biol.* **1999**, *6*, 28.
(49) Kozar, N.; Schreiber, G. Effect of crowding on protein-protein association rats: fundamental difference between low and high mass vrowding agents. *J. Mol. Biol.* **2004**, *336*, 763−774.
(50) Phillip, Y.; Sherman, E.; Haran, G.; Schreiber, G. Common crowding agents have only a small effect on protein-protein interactions. *Biophys. J.* **2009**, *97*, 875−885.
(51) Zhou, H.-X. Protein folding and binding in confined spaces and in crowded solutions. *J. Mol. Recognit.* **2004**, *17*, 368−375.
(52) Minton, A. P. Excluded volume as a determinant of macromolecular structure and reactivity. *Biopolymers* **1981**, *20*, 2093−2120.
(53) Grote, R. F.; Hynes, J. T. The stable states picture of chemical reactions. II. Rate constants for condensed and gas phase reaction models. *J. Chem. Phys.* **1980**, *73*, 2715−2732.
(54) Velsko, S. P.; Fleming, G. R. Photochemical isomerization in solution. Photophysics of dipheny butadiene. *J. Chem. Phys.* **1982**, *76*, 3553−3562.
(55) Velsko, S. P.; Waldeck, D. H.; Fleming, G. R. Breakdown of Kramers theory description of photochemical isomerization and the possible involvment of frequency dependent friction. *J. Chem. Phys.* **1982**, *78*, 249−258.
(56) Bagchi, B.; Oxtoby, D. W. The effect of frequency dependent friction on isomerization dynamics in solution. *J. Phys. Chem.* **1983**, *78*, 2735−2741.

https://doi.org/10.1021/acs.jpcb.3c04070
J. Phys. Chem. B 2023, 127, 8095−8105